Searching for comets encountering Jupiter.

Second campaign observations and further constraints on the size of the Jupiter family population[*]

M. Lindgren[1], G. Tancredi[2], C.-I. Lagerkvist[1] and O. Hernius[1]

[1] Astronomical Observatory, Box 515, 751 20 Uppsala, Sweden
[2] Depto. de Astronomia, Facultad de Ciencias, Tristan Narvaja 1674, 11200 Montevideo, Uruguay

Abstract. — The results from the second campaign of the search for comets in the vicinity of Jupiter are presented. As in the previous campaign, we find no comets. This result is used to calculate upper limits on the size of the Jupiter family population of comets. The numbers found are the same as in the previous campaign, but have the advantage that the lack of complete discovery at the limiting magnitude is taken into account. We find that for comets brighter than nuclear B magnitude 14 (corresponding to a radius of 8 km) the population consist of up to 210 members. This value is extrapolated to fainter magnitudes (smaller sizes).

1. Introduction

This is a presentation of the results from the second comet search in the vicinity of Jupiter. The first campaign was conducted in 1992, and the results have been presented in Tancredi & Lindgren (1994; hereafter TL94). The main feature of this search is that, by looking towards Jupiter in opposition, it is not only possible to increase the probability of finding a comet, it is also easier to identify any found object as a comet (active or dormant) due to the fact that no other known population of small bodies occupy the volume of space covered in the search. The strategy for this project was outlined by Tancredi & Lindgren (1992, hereafter TL92).

In the 1992 campaign (TL94), 36 Schmidt plates were obtained at ESO in March 1992. The limiting magnitude of the plates was such that it corresponded to inactive comets with nuclear magnitude $B < 13.8$. No comets were found, but this result was used together with a model (based on numerical integrations of the known Jupiter family) for the probability of finding a comet in the vicinity of Jupiter, to make an upper estimate of 210 comets with nuclear magnitude $B \leq 13.8$ for the whole popula-

tion of Jupiter family comets. This upper limit was then extrapolated to fainter magnitudes.

The results from the second campaign in 1993 will be presented here. As in 1992, no comets were found, but we will show that the increased probability of finding an object can be used to further constrain the population of Jupiter family comets.

The observations were made in the same manner as in 1992, and are presented in Sect. 2 together with the reductions. The results and the analysis of these are found in Sects. 3 and 4. A discussion of the results and a future outlook are found in Sect. 6.

2. Observations

2.1. *The plates*

37 photographic plates and films were obtained in March and April 1993 with the Schmidt telescopes at the European Southern Observatory (March) and the UK Schmidt telescope at the Anglo-Australian Observatory (April).

The investigated region around Jupiter was covered with nine plate-fields. Since each plate-field covers an area of $5°.4 \times 5°.4$ on the sky, the area covered in the campaign is approximately $16° \times 16°$. The central plate field was centered on Jupiter's position. The covered region is therefore centered slightly off the ecliptic as the ecliptic latitude of Jupiter was $+1°.3$ at the time of the observations.

Each plate-field was exposed on three different observing nights during one week in March 1993. This was done with the purpose to easily link the moving objects from one observing night to the next. To obtain reliable orbital elements, follow-up observations were carried out during the next new moon period in April 1993. The central coordinates of the April sky field were shifted by about 6° to the west to compensate for one month of motion of the moving objects found on the March plates.

The March plates were exposed for 105 minutes, using the apparent motion of Jupiter ($18\rlap{.}''8°\mathrm{h}^{-1}$) as tracking rate; the extra 15 minutes (as compared to the 1992 exposure time of 90 minutes) being added to facilitate a 15 minute closure of the telescope shutter after 60 minutes exposure. Each object then produces two trails, the first one twice as long as the second. This tracking approach helps to identify the moving objects as the short end of the trail for a moving object generally points in the opposite direction to the short end of a star trail. The April plates and films were exposed for 45 minutes using sidereal tracking rate.

Table 1 gives the plate center coordinates. All plates have a IIIa-J hypersensitized emulsion and were exposed through a blue cut-off filter (GG385). The observing conditions were better during the 1993 observations, compared with the 1992 conditions, since the central region then culminated at an altitude of 65° above the local horizon, as compared with 50°, and the average seeing during the 1993 observations was $1\rlap{.}''0$, compared to $1\rlap{.}''5$ in the 1992 campaign.

Table 1. Plate center coordinates (J2000.0) for the 1993 plates and films

Plate field	Date of exposures	α	δ
1	1993 March 16,17,22	$12^{\mathrm{h}}23^{\mathrm{m}}$	$+2°21'$
2	1993 March 16,17,22	$12^{\mathrm{h}}44^{\mathrm{m}}$	$+2°21'$
3	1993 March 16,17,22	$13^{\mathrm{h}}04^{\mathrm{m}}$	$+2°21'$
4	1993 March 18,19,23	$12^{\mathrm{h}}23^{\mathrm{m}}$	$-3°00'$
5	1993 March 18,19,23	$12^{\mathrm{h}}44^{\mathrm{m}}$	$-3°00'$
6	1993 March 18,19,23	$13^{\mathrm{h}}04^{\mathrm{m}}$	$-3°00'$
7	1993 March 20,21,25	$12^{\mathrm{h}}23^{\mathrm{m}}$	$-8°15'$
8	1993 March 20,21,25	$12^{\mathrm{h}}44^{\mathrm{m}}$	$-8°15'$
9	1993 March 20,21,25,26	$13^{\mathrm{h}}04^{\mathrm{m}}$	$-8°15'$
1	1993 April 16	$12^{\mathrm{h}}01^{\mathrm{m}}$	$+4°26'$
2	1993 April 16	$12^{\mathrm{h}}26^{\mathrm{m}}$	$+4°26'$
3	1993 April 16	$12^{\mathrm{h}}53^{\mathrm{m}}$	$+4°26'$
4	1993 April 17	$12^{\mathrm{h}}01^{\mathrm{m}}$	$-1°48'$
5	1993 April 21	$12^{\mathrm{h}}26^{\mathrm{m}}$	$-1°48'$
6	1993 April 18	$12^{\mathrm{h}}53^{\mathrm{m}}$	$-1°48'$
7	1993 April 17	$12^{\mathrm{h}}01^{\mathrm{m}}$	$-8°03'$
8	1993 April 17	$12^{\mathrm{h}}26^{\mathrm{m}}$	$-8°03'$
9	1993 April 18	$12^{\mathrm{h}}53^{\mathrm{m}}$	$-8°03'$

2.2. *Plate reductions*

Positions:

All plates and films were scanned manually at least three times. Around 8000 trails of moving objects were found and measured with the OPTRONICS measuring system at ESO headquarters in Garching.

For the April 1993 films an automatic scanning was done with the COSMOS scanning device at the Edinburgh Observatory. However, a re-measurement had to be done for parts of the films since the scanning was incomplete and not optimized for moving objects. The re-measuring was done at the Geographic Institute, Uppsala, using a digitizing table. The accuracy of this device is not as good as for the OPTRONICS system, but was considered to be adequate. COSMOS positions have been used when available.

Due to the relatively large size of the Schmidt-plates, $5\rlap{.}°4\times5\rlap{.}°4$, it is difficult to obtain a high positional accuracy over the entire plate with a single reduction. The reduction procedure was thus performed separately for different parts of the plates. However, the mean accuracy for the whole area of the plate, is well below $1''$ in both right ascension and declination, as Table 2 shows, and can be accounted for by errors in the PPM and SAO star catalogues. The mean numbers of PPM and SAO reference stars used in the reduction of the positions are also given in the table.

Table 2. Average quality (mean standard deviation) of the positions on the plates. The values for April are mean values based on two subsets of measurements: 50% measured with an accuracy similar to the March values, and 50% measured with an accuracy $\sim 2.5''$

	$\overline{\sigma_\alpha}$	$\overline{\sigma_\delta}$	Ref. stars
March	$0\rlap{.}''68$	$0\rlap{.}''58$	27
April	$1\rlap{.}''5$	$1\rlap{.}''5$	53

After measuring all trails it is possible to examine the distribution of apparent motions. The arguments for using this strategy (TL92) included the point that the apparent motion relative to Jupiter of comets in the vicinity of the planet should be smaller than for asteroids and stars in the same direction, and comparable to the relative motion of the Jovian satellites. Figure 1 is a plot of $(\mathrm{d}\alpha/\mathrm{d}t, \mathrm{d}\delta/\mathrm{d}t)$, and should be compared with Fig. 2. The circle defines the region of angular velocity in which we can expect Jupiter-encountering comets. The dots with small circles are Jovian satellites.

We see that our measured apparent motions cluster with the same pattern as for the numbered asteroids. There are a few objects with apparent motions within the circle which surrounds the region where comets should

show up. However, taking the errors in the measurements, shown in the figure, into consideration it is doubtful that they can be considered as comet candidates, and it was not possible to calculate reliable orbits for any of these objects.
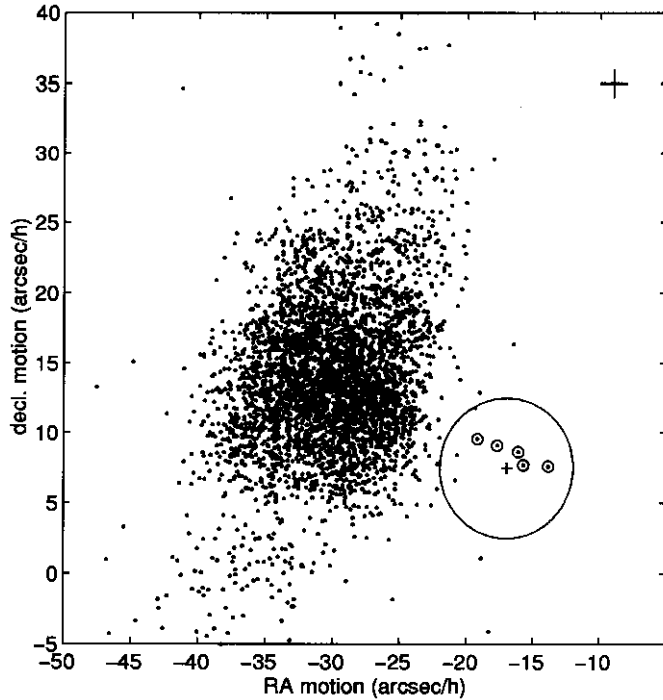

Fig. 1. Apparent motion of all measured trails. The small + in the center of the circle represents Jupiter, and the small circles the Jovian satellites. The big circle defines the region in which Jupiter-encountering comets are to be expected. The error bar in the upper right corner indicates the error in the measurement of the apparent motion

Linking:

The linkings of the March exposures were done by trail-identification using the length, position, angle and brightness of the trails. The trails were linearly extrapolated from one exposure to the next and in most cases it was obvious which trails belonged to the same object. About 55% of the objects could be detected on two plates and about 40% on three plates. Those that were found only once or twice are generally faint and were lost mainly because of different seeing conditions during the different observing nights.

It was not possible to predict the positions on the April exposures by a linear extrapolation of the March trails. The motion in right ascension and declination cannot be approximated with a straight line on longer time-scales. To make the search for the fourth (April) position as easy as possible, we added a fictitious fourth position, chosen as the continuation of the approximately linear March mo-
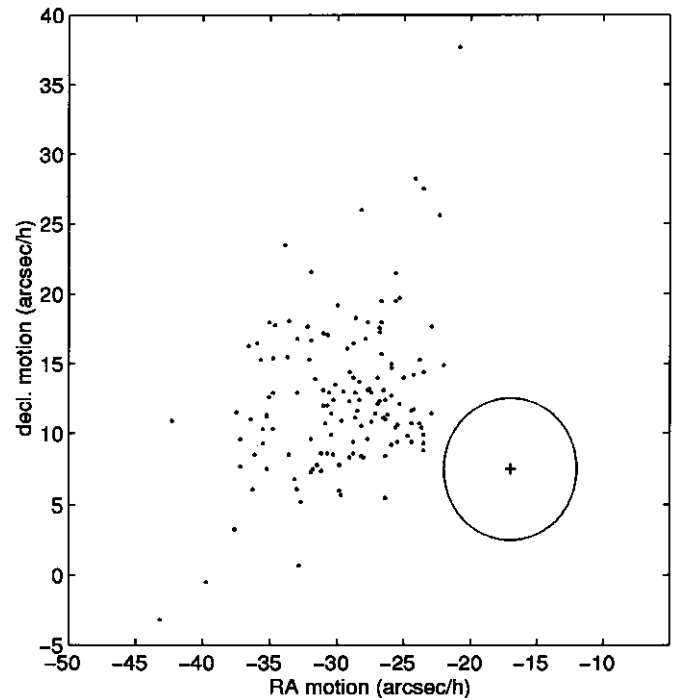

Fig. 2. Hourly motion in α and δ of all numbered asteroids (small dots) and Jupiter for the 1993 campaign. This figure is similar to Fig. 6 in TL92

tion until the April date, and calculated an orbit using only the three March positions. The orbit determination outputs residuals in right ascension and declination for the fourth fictitious position, indicating where the real fourth position (trail) should be on the plate. This seemingly cumbersome procedure has the advantage that it is not necessary to calculate an ephemeris for each object, and in our case with thousands of measured positions, it means a big reduction of time needed to do the linkings. About 15% of all objects found on the March plates could be recovered on the April plates. The objects that were not found were either outside the field of view or too faint to be detected.

Orbit determinations:

The linkings of the trails were confirmed by G.V. Williams at the Minor Planet Center (private communication), as well as extended to include older observations. The orbit determination was also made independently by Williams, and at the moment some 1500 objects have been designated a preliminary orbit. The bulk of these can be found in MPC 23379–23477 and MPC 23578–23633.

The few "suspect" objects with short trails, found within the expected region in Fig. 1 have very uncertain orbit determinations, and are thus not considered as reliable comet candidates.

2.3. Limiting magnitude

In the 1992 campaign it was found that the limiting magnitude for stationary (point source) objects, was $B = 22.1$. This number was found by comparisons with photometric standard stars and Jupiter satellite JXIII Leda. Some care was taken to find the effect of trailing on the limiting magnitude, and it was shown that the correction (Δm) to the limiting magnitude follows the expression (Eq. (4) and Fig. 3 in TL94):

$$\Delta m = -2.5 \log\left[\frac{\ell/d}{1.06\mathrm{erf}(0.83\ell/d)}\right] \quad (1)$$

where ℓ/d is the length of the trail, expressed in units of the width of the seeing disk, and erf is the error function. This resulted in a limiting magnitude for slow-moving objects ($4''\mathrm{h}^{-1}$) of $B = 20.7$ (TL94).

In the 1993 campaign we had no possibility to expose any photometric standard stars, and the seeing conditions were so much better, that J XIII Leda was not on the limit of detection (as it was in the 1992 campaign), and hence useless as indicator of the limiting magnitude. However, it should be noted that all conditions regarding the observations and the reductions (i.e. plates, filters, exposure times, method of scanning etc.) were identical between the two campaigns. The only differing factor is the width of the seeing disk: in 1992 the seeing was 1.5 arcsec, and in 1993 it was 1.0 arcsec. Based on this fact, and using the average relative angular velocity of $4''\mathrm{h}^{-1}$ in TL94, it is possible to extrapolate, by using Eq. 1, to a "theoretical" limiting magnitude for slow-moving objects in the 1993 campaign. Doing this, we get a difference of +0.4 magnitudes compared to the limit in the 1992 campaign. Hence the value $B = 21.1$ is the limiting apparent magnitude for the slow-moving objects in the 1993 campaign.

Another way of finding the limiting magnitude of the 1993 campaign is to make use of the magnitude distribution actually determined in both campaigns. Although the method used to measure the apparent magnitudes (Lagerkvist et al. 1995) is rather crude, and not very reliable for faint objects, it is possible to take advantage of the fact that the cumulative distributions of the apparent magnitudes in the campaigns reflect the same underlying population, and should therefore be identical. It was found (van Houten et al. 1970) that the distribution of the apparent magnitudes follows a power law:

$$N(\leq m) \propto 10^{-\alpha m} \quad (2)$$

where $N(\leq m)$ is the number of objects brighter than apparent magnitude m, and α the index. Figure 3 shows the distributions for both campaigns. The magnitudes used for each object is the measured apparent magnitude as described in Lagerkvist et al. (1995). Shown together with the data points is a least-squares-fitted power law with index 0.6. The fit is made for objects in the magnitude

interval 15–17, since that interval contains the most reliable magnitude estimates, while not risking to overlap the limit of completeness. The distribution in Fig. 3 contains a total of 2559 and 3984 objects, for the 1992 and 1993 campaigns, respectively. Inserting these numbers into Eq. (2) we get:

$$\log(2559) - \log(3984) = -0.6\Delta m_{\mathrm{II-I}} \quad (3)$$

where $\Delta m_{\mathrm{II-I}}$ is the difference in limiting magnitude. The numerical value becomes $\Delta m_{\mathrm{II-I}} = 0.3$, in rough agreement with the "theoretical" difference found above. Although the magnitudes determined are V magnitudes, the value of Δm is still the same, since there is no big systematic trend of $B - V$ color with V. Note that this difference is not applicable for stationary objects, since the calculation is made using the magnitude distribution for moving objects. The estimate is still valid since the erf function for asteroids and slow-moving objects is almost 1, and thus $\Delta m_{\mathrm{II-I}}$ is independent of the trail length.
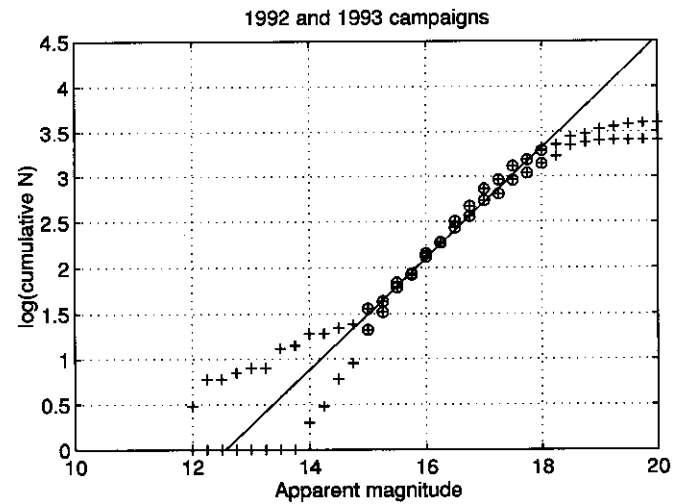

Fig. 3. The cumulative distribution of objects found in the 1992 and 1993 campaigns, as a function of apparent magnitude. All objects with measured magnitude have been used. The straight line is a least-squares-fit to the encircled points, with slope 0.6

2.4. Completeness of the search

With the distribution of the magnitudes in hand we can make an estimate of the completeness of the search, as a function of magnitude. Figure 4a shows the cumulative distribution of apparent V magnitude for the objects found in the 1993 campaign. The magnitudes of these objects have all been shifted in magnitude using Eq. (1), corresponding to their respective relative angular motion with respect to Jupiter, and thus represent magnitudes of stationary (point source) objects . The straight line is

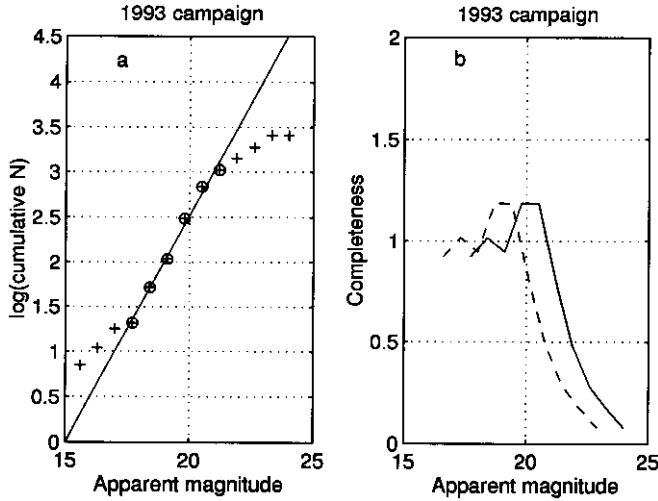a least-squares-fit in the interval corresponding to where good calibration exists (Lagerkvist et al. 1995).

Fig. 4. The cumulative distribution of the number of objects found in the 1993 campaign, as a function of point source V magnitude is shown in panel **a)**. The straight line is a least-squares-fit to the points in the magnitude interval where the accuracy is reliable. Panel **b)** shows the corresponding completeness (solid line). The dashed line is shifted in magnitude the distance corresponding to slow-moving comets in the 1993 campaign. The data points in panel **b)** for the brighter magnitudes have been omitted due to the small numbers involved

Define the completeness for objects brighter than magnitude m as:

$$C(<m) = \frac{\text{Number of objects detected}}{\text{Number of objects estimated}} \qquad (4)$$

where the estimated number of objects is calculated using a fitted power-law (Eq. 2) shown in Fig. 4a. Figure 4b shows the result, that for stationary objects with apparent V magnitudes brighter than ~ 21, the detection of objects is more or less complete, and for fainter magnitudes completeness is a decreasing function of the magnitude, going down to zero at about $V = 24$.

We can get the corresponding function for comets in the vicinity of Jupiter by shifting the completeness function with a Δm-value corresponding to the trail length of slow-moving objects and correcting for the $B - V$ color. Using a mean apparent angular motion of $4''\text{h}^{-1}$ for slow-moving objects found in TL92, and inserting into Eq. (1) we get $\Delta m = 1.9$. Assuming, as in TL94, that the $B - V$ color of the comets is 0.8 we get 100% completeness for comets brighter than $B = 21 + 0.8 - 1.9 = 19.9$, and a completeness of 40% for comets brighter than the limiting magnitude $B = 21.1$ found in Sect. 2.3.

The corresponding calculation for the 1992 campaign can also be made, since we now have estimates of the magnitudes of all trails for that campaign as well. Figure 5a shows the cumulative number of objects as a function of
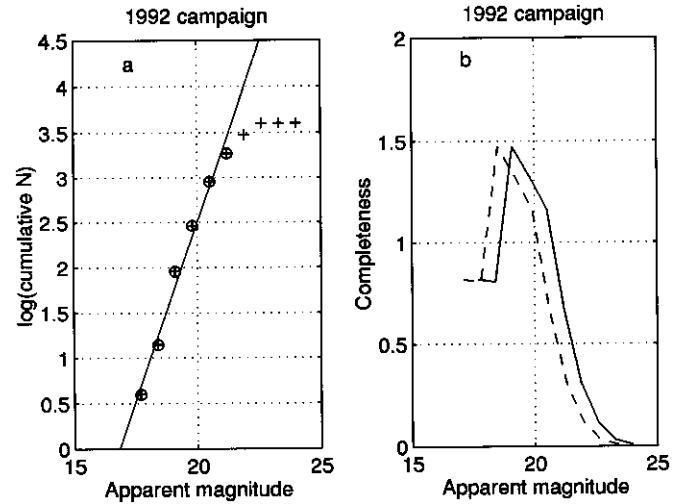

Fig. 5. The cumulative distribution of the number of objects found in the 1992 campaign, as a function of point source V magnitude is shown in panel **a)**. The straight line is a least-squares-fit to the points in the magnitude interval where the accuracy is reliable. Panel **b)** shows the corresponding completeness (solid line). The dashed line is shifted in magnitude the distance corresponding to slow-moving comets in the 1992 campaign. The data points in panel **b)** for the brighter magnitudes have been omitted due to the small numbers involved

V magnitude, and Fig. 5b the corresponding completeness function. Shifting the completeness in Fig. 5b by the corresponding 1992 value for $\Delta m = 1.4$ and $B - V = 0.8$ leads to a completeness of 100% for $B = 19.4$, and a completeness of 60% for the limiting B magnitude 20.7.

3. Results from the second search for comets

To summarize the results from the second search for comets in the vicinity of Jupiter, we find that no slow-moving object brighter than apparent B-magnitude 21.1 was found.

However, it should be mentioned that there was one comet in the field of view of this search. The split comet D/Shoemaker-Levy 9 was spotted on March 21 by one of the authors (M.L.) while scanning one of the March 19 plates. However, he did not report the discovery until after the official discovery by the Shoemaker-Levy team, as communicated by Marsden (1993).

Although a comet, by definition, and definitely in the vicinity of Jupiter, this object falls outside of our scope for this search strategy. We were looking for inactive or barely active nuclei, a typical situation for a JF comet at 5 AU from the Sun. D/Shoemaker-Levy 9 at the time of the 1993 observations had brightened by many magnitudes due to the fragmentation, which occurred in July 1992, after our last observations in April 1992. As we reported in TL94, the comet was not found on any of our plates, and based on that we can estimate an upper limit to its brightness

and size: nuclear magnitude fainter than $B(1,0)=14.3$ and radius smaller than 7.2 km (for a geometrical albedo of 0.03).

4. Analysis

4.1. The 1993 campaign by itself

We use the same method of analysis as in TL94. The probability for a Jupiter family comet to be present in the vicinity of Jupiter, within a distance D (AU) from the planet was found to be (Fig. 6 and Eq. (6) in TL94):

$$\overline{p}(D) = 0.014\,D^{2.5} \quad (5)$$

where the factor 0.014 is the mean probability, averaged for orbits with perihelion distance in the range $1.5 < q < 4.5$ AU (Fig. 5 in TL94). By integrating the differential probability, found by differentiating the cumulative probability in Eq. (5), over the volume of space covered in the search, we get

$$p_V = \frac{2.5 \cdot 0.014}{4\pi} \int_V \frac{1}{\sqrt{D}} dV \quad (6)$$

where V is the "truncated pyramid" defined by a square in the sky-plane of $16°.2 \times 16°.2$ and an outer (spherical) surface chosen based on the distribution of aphelion distances (Q) of the Jupiter family: the outer "edge" of the distribution at 6.8 AU. The inner (spherical) surface is given by the heliocentric distance at which the outermost object was found in this search. Figure 6 shows the distribution, and the value chosen is 4.0 AU. Numerical integration of Eq. (6) yields the same value as in TL94, $p_V = 0.014$, which is used to calculate the upper limit on how many objects that can be present in the volume, while still being consistent with a number of zero observed objects. The probability of an event defined by observation of a number x objects is described by the Poisson distribution:

$$P(x) = \frac{\lambda^x e^{-\lambda}}{x!} \quad (7)$$

where λ is the parameter, defined as the expected number of occurrences of the event during the time in consideration. In our case $\lambda = np_V$, where n is the population size. Then, $P(0) = e^{-\lambda}$. Inserting the value for p_V, and using the fact that $\sum_x P(x) = 1$, we find that with a probability of 0.95, $n \leq 210$.

What this number tells us is that, down to our limiting apparent magnitude, the Jupiter family contains no more than 210 comets. But, as in TL94, we must interpret this in terms of absolute magnitude and size, as well as consider the case where a part of the population is brightened by some cometary activity.

First, we consider the case of non-active comets. Then the relation between absolute and apparent magnitude is purely a geometric correction:
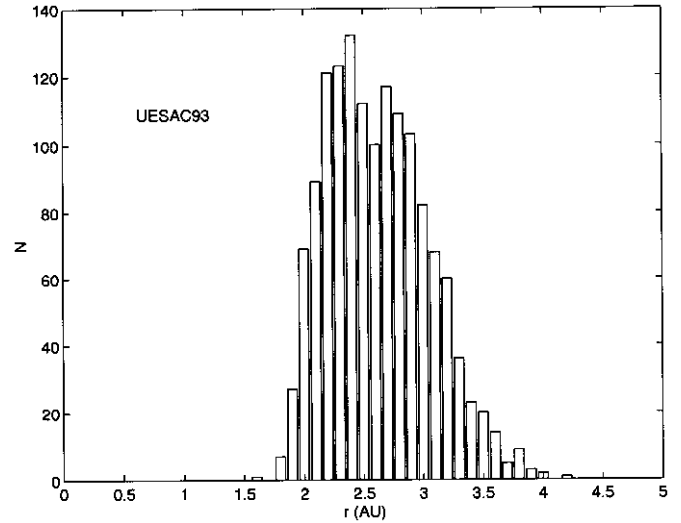

Fig. 6. The distribution of heliocentric distances at which the asteroids in the 1993 campaign were found. The calculation is based on 1433 successfully determined orbits

$$H_N = m - 5\log(r\Delta) - \beta\alpha \quad (8)$$

where H_N is the absolute nuclear magnitude, m is the apparent magnitude, r and Δ are the heliocentric and geocentric distances, respectively, and α and β are the phase angle and the phase coefficient. Using the value 0.035 for the phase coefficient found by Jewitt (1991) and the mean values of r and Δ in the volume, given by:

$$\langle r \rangle = \frac{\int_V r\,dV}{\int_V dV} \quad (9)$$

and

$$\langle \Delta \rangle = \frac{\int_V \Delta\,dV}{\int_V dV} \quad (10)$$

we get 5.68 AU, 4.68 and 2° for $\langle r \rangle$, $\langle \Delta \rangle$ and α respectively, we get $H_N = m - 7.1$. By inserting the limiting apparent magnitude for the search, $B = 21.1$, we get the limiting absolute nuclear magnitude, $H_N^B = 14.0$, which corresponds to a diameter of 8 km if we use a typical geometric albedo of 0.03 (Jewitt 1991).

The other alternative to interpret the apparent limiting magnitude, is to consider that a certain fraction of the comets are active (and hence brightened) at the heliocentric distance in question. This was discussed in some detail in TL94, and we will make use of it in Sect. 5 below, where we extrapolate the upper limit on the number of comets to fainter absolute magnitudes.

4.2. Combining the two campaigns

The main reason for pursuing this second campaign is that by repeating the observations, following the same procedure, we increase the probability and can get a better constraint on the population size. As we will show below, the mean duration for a comet to be in the vicinity of Jupiter is slightly longer than the time between the two campaigns, with the consequence that the "combined" neighboring probability increases to such a degree that we can constrain the population considerably.

Duration of encounters:

From the numerical integrations of the Jupiter family of comets in TL92 we can extract the duration of each encounter with Jupiter. Figure 7 corresponds to the dotted line in Fig. 5 in TL92. Each point on the curve is the mean value of the duration, defined as the time the comet stays within a distance D (AU) from the planet. As the figure shows, the points can be least-square-fitted to a straight line:
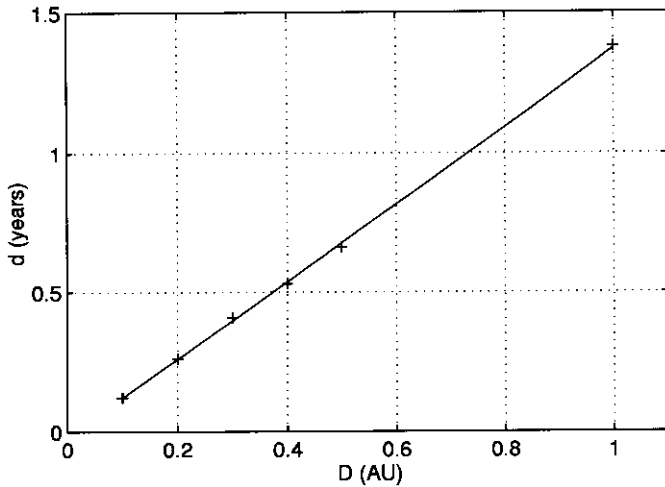
$$d(D) = 1.4D \text{ years} \tag{11}$$

Fig. 7. The duration of encounters (d) as a function of the distance (D) which defines the entry into each encounter. The duration is the time the comet spends within the distance D. The crosses are mean values based on data for orbits with q in the range $1.5 \leq q \leq 4.5$ AU, and the line is a least-squares-fit to the points. All values are derived from the numerical integrations presented in TL92

The mean value of the duration of a visit within the volume is not easy to calculate. We can find a good approximation by finding the mean distance $\langle D \rangle$ of points on the bounding surfaces. This we do by calculating:

$$\langle D \rangle = \frac{\int_S D \mathrm{d}S}{\int_S \mathrm{d}S} \tag{12}$$

where $\int_S$ is the surface integral over the surface bounding the volume. We approximate the volume by a rectangular box with sides corresponding to the measures given for V above. This evaluates to $\langle D \rangle = 1.1$ AU, and inserting into Eq. (11) we get $\langle d \rangle = 1.5$ years.

This means that the fraction f of the number of comets in the vicinity of Jupiter in the 1992 campaign, that is still in the vicinity, is approximately given by

$$f \sim 1 - \frac{\Delta t}{\langle d \rangle} = 0.30 \tag{13}$$

where we have used that Δt (the interval between the two campaigns) is 1.05 years.

Adding the probabilities:

Define $e92$ and $e93$ as the events of finding a comet in the 1992 and 1993 campaigns respectively, and $P(e92)$ and $P(e93)$ their corresponding probabilities. The additive law of probability gives us then the probability to find an object in the combined campaign:

$$P = P(e92 \cup e93) = P(e92) + P(e93) - P(e92 \cap e93) \tag{14}$$

where $P(e92 \cap e93)$ is the probability to find an object in both campaigns. Using the fact that $P(e92) = P(e93)$ and inserting $P(e92 \cap e93) = P(e92) \cdot f$, we get:

$$P = 2P(e92) - P(e92) \cdot f = P(e92) \cdot (2 - f) \tag{15}$$

This "combined" P can then be used, as above, to get a new limit on the number of comets encountering Jupiter. Inserting the numerical values, we get $P = 0.024$, and by using Eq. (7), the corresponding $n \leq 125$.

It must be remembered that this limit is valid only for the magnitude interval common to the two campaigns, i.e. $B \leq 20.7$. Although this is an interesting number, we have not yet used the fact that the 1993 campaign has a fainter limiting magnitude. However, the different limiting magnitudes in the two campaigns makes the interpretation difficult. We have no knowledge about the combined probability p_V between the two different limiting magnitudes of the campaigns. All we know is that, at $B = 20.7$ the combined probability given by Eq. (15) is 0.024, and at $B = 21.1$ the combined probability is zero.

Nevertheless, if we make use of a model for the magnitude distribution, we can get a limit on the population by extrapolation down to the fainter magnitude limit in the 1993 campaign. This procedure will be discussed below in Sect. 5, together with the extrapolations we make to find the total population of Jupiter family comets for fainter absolute magnitudes (smaller nuclear sizes).

4.3. Correcting for the completeness

In TL94 we did not know the number distribution as a function of magnitude for the objects in the 1992 campaign since we at the time did not have any measurements of their magnitudes. This meant that we could not estimate to what degree the search was complete down to our limiting magnitude. However, as discussed above (Sect. 2.4) we can now estimate a 60% completeness for objects brighter than $B = 20.7$ in the 1992 campaign. And by looking at Fig. 4 in the present campaign we find the same value at that magnitude. Thus for the $B = 20.7$ limit we use a completeness of 60%, and for the limit $B = 21.1$ a completeness of 40%.

To summarize, so far we have presented the results from the observations without making any extrapolations, and before proceeding it is appropriate to clarify these. Table 3 shows the numbers found so far, corrected for the respective completeness factor $(1/C)$. Note that these upper limits are independent of any fraction of the population being active (and thus brightened). That is, the inequality $210 \geq N = N_{\mathrm{a}} + N_{\mathrm{d}}$ holds together and separately for the two populations, N_{d} and N_{a}, consisting of dormant and active comets respectively.

5. A new limit on the population size

As discussed in TL94, the distribution of nuclear magnitudes for comets follows a power law with an index s:

$$N(< H_N) \propto 10^{s H_N} \qquad (16)$$

where $N(< H_N)$ is the cumulative number of comets brighter than nuclear magnitude H_N. Arguments have been presented for indices in the range $0.3 \leq s \leq 0.5$ (TL94 and Refs. therein). We will estimate the upper limits on the total population using these.

In the 1992 campaign, the observing geometry in combination with the limiting apparent magnitude led to a limiting absolute nuclear magnitude of $H_N^B = 13.8$, corresponding to a nuclear radius of 9 km. As shown above (Sect. 4.1), the present campaign reaches a nuclear magnitude of $H_N^B = 14.0$, corresponding to a radius of 8 km. This means that if we want to use the limits based on the combination of the two campaigns, presented in Table 3, to constrain the Jupiter family population of smaller comets, we can only utilize the limit set on the subset of comets brighter than $H_N^B = 13.8$ for the extrapolation. However, the limit calculated for $H_N^B \leq 14.0$ (corresponding to $B \leq 21.1$) was found to be 520 (Table 3), thus constraining the population for comet sizes down to a radius of 8 km. If we extrapolate the upper limit found for the combined probability at $H_N^B = 13.8$ to a magnitude of 14.0, we get values ranging from 240 to 265, depending on the s-indices. We then conclude that the limit set by the combination of both campaign, though referring to a brighter magnitude, is a better constraint on the size

of the population compared to the fainter limit of 1993 campaign by itself.

Following TL94, the extrapolations of the limits to fainter magnitudes have been made, using the different s-indices. The results are shown in Fig. 8, and should be compared with Fig. 8 in TL94.

Based on the same observational data set (regarding the level of activity for comets at the distance of Jupiter) as referred to in TL94, we calculate upper limits on the population, with the assumption that half the number of comets at the heliocentric distances in question ($\gtrsim 4$ AU) are active to some degree. The dashed lines in Fig. 8 correspond to a 50% fraction of the total Jupiter family population brightened by 1.5 magnitudes.
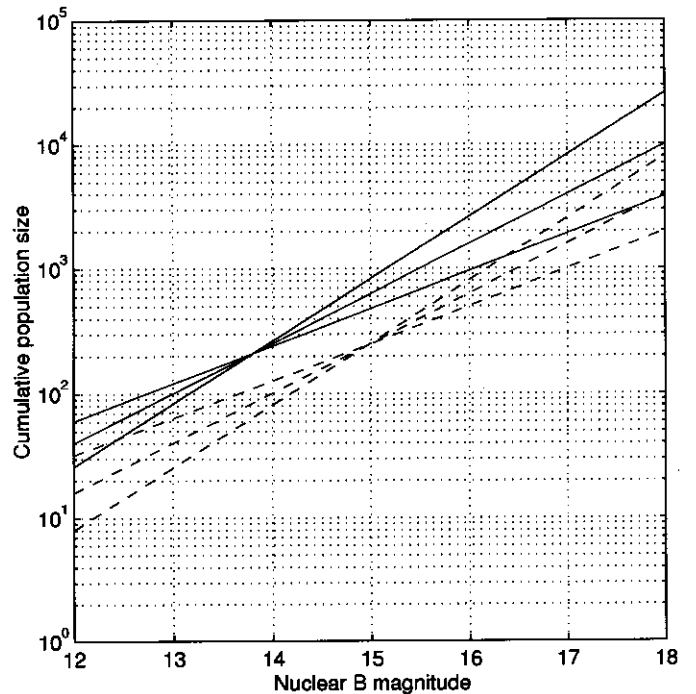

Fig. 8. Upper limits on the population size. Solid lines correspond to the situation where all comets are inactive, and dashed lines show the limits if 50% of the comets are brightened by 1.5 magnitudes due to activity. The steepest lines correspond to a power law index of 0.5 and the flattest to an index of 0.3

It can be seen that for a nuclear B magnitude of 18 (corresponding to a radius of 1.3 km if a geometric albedo of 0.03 is assumed) the upper limit on the population is on the same order as the previous estimate in Fig. 8 of TL94, but now the limits are much firmer due to the fact that we have compensated for the completeness of the search. Table 4 summarizes the results. The middle section of the table shows the upper limits on a population that may consist either of a combination of active and dormant comets, or only active or dormant comets separately, as explained by the relation $210 \geq N = N_{\mathrm{a}} + N_{\mathrm{d}}$ shown above. The right

Table 3. A summary of the upper limits on the number of comets found in the comet search campaigns of 1992 and 1993. B is the blue magnitude, and N is the completeness adjusted upper limit on the number of comets in the Jupiter family. The numbers in parentheses are the uncorrected values. C is the completeness factor used to correct the values

B limit	N limit	C	Notes
$B \leq 20.7$	$N \leq 350$ (210)	0.6	1992 and 1993 campaigns separately
$B \leq 20.7$	$N \leq 210$ (125)	0.6	Combined 1992 and 1993 campaign
$B \leq 21.1$	$N \leq 520$ (210)	0.4	1993 campaign

hand section shows the limits on a population in which half of the members are brightened by 1.5 magnitudes.

Table 4. Summary of the upper limits on the Jupiter family population, as presented in Fig. 8. $H_N^B = 13.8$ corresponds to a nuclear radius of 9 km, and $H_N^B = 18.0$ to a radius of 1.3 km

H_N^B	N (dormant/active)			N limit (50% active)		
	$s=0.3$	$s=0.4$	$s=0.5$	$s=0.3$	$s=0.4$	$s=0.5$
13.8	210	210	210	110	84	64
18.0	3900	10000	27000	2000	4000	8000

6. Conclusions

Inspecting the results in Table 4, we see that the numbers coincide with the numbers found in TL94 from the first campaign. However, the present limits are considerably firmer, in view of the fact that we have taken the completeness factor into consideration. In the 1992 campaign, presented in TL94, we had no possibility to measure the magnitudes of the objects (asteroids) found. This forced us to (implicitly) assume a 100% completeness of that campaign. Now we have estimates of the magnitudes of thousands of asteroids, leading to a more reasonable estimate of the completeness factor, and we see that the numbers in TL94 should have been corrected by almost a factor 2 upwards.

To improve the results, it is obvious that we need to reach fainter magnitudes. The limiting magnitude of this search corresponds to large comet nuclei (8−9 km radius). The limits set on smaller nuclei, the ones more consistent with the observed Jupiter family comets, are only extrapolations. But to reach apparent magnitudes corresponding to these sizes, we must utilize more sensitive detectors than photographic emulsions. The obvious solution is of course to use modern CCD detectors. But as long as the size of a CCD detector is on the order of 1% of a photographic plate we are forced to conclude that we probably have to wait some time before we can make a big improvement on the present results.

References

Jewitt D., 1991, Cometary photometry, in "Comets in the post-Halley era" Vol. 1. In: Newburn Jr. R.L., Neugebauer M. and Rahe J. (eds.). Kluwer, Dordrecht, pp. 19–65

Lagerkvist C.-I., Hernius O., Lindgren M., Tancredi G., 1995, UESAC – The Uppsala-ESO survey of asteroids and comets, in "Third international workshop on positional astronomy and celestial mechanics". In: López Garcia A. (ed.), Valencia (in press)

Marsden B.G., 1993, IAU Circular 5725

Tancredi G., Lindgren M., 1992 (TL92), The vicinity of Jupiter: a region to look for comets, in "Asteroids, Comets, Meteors 1991". In: Harris A. and Bowell E. (eds.), Lunar and Planetary Institute, Houston, pp. 601–604

Tancredi G., Lindgren M., 1994 (TL94), Searching for comets encountering Jupiter: First campaign, Icarus 107, 311–321

van Houten C.J., van Houten-Groeneveld I., Herget P., Gehrels T., 1970, A&AS 2, 339–448